3566 *Macromolecules* **2010**, *43*, 3566–3569
DOI: 10.1021/ma1002134

Macromolecules
NOTE

Polylactide−Polythiophene−Polylactide Triblock Copolymers

Bryan W. Boudouris,[†] **C. Daniel Frisbie,***[,†] **and Marc A. Hillmyer***[,‡]

[†]*Department of Chemical Engineering and Materials Science and* [‡]*Department of Chemistry, University of Minnesota, Minneapolis, Minnesota 55455-0431*

Received January 27, 2010; Revised Manuscript Received February 23, 2010

Introduction

Soluble polythiophene derivatives, such as poly(3-alkylthiophenes) (P3ATs), have broad application in organic electronics because they transport holes efficiently (μ_h ~0.1−1 cm^2 V^{-1} s^{-1}), are processable into films from many organic solvents, and they exhibit relatively low band gaps (E_g ~1.9 eV) that can be tuned by chemical modification.[1−4] In particular, thiophene-containing electron donor polymers in combination with electron-accepting fullerenes are employed widely in high performance, bulk heterojunction (BHJ) organic photovoltaic cells (OPVs) that exhibit power conversion efficiencies as high as ~5−6%.[5−7] Because the photoexcited electron−hole pairs (excitons) in BHJ OPVs dissociate into free charge carriers most usefully at the electron donor−acceptor interfaces, the morphology of polythiophene/fullerene active layers is crucial to device performance.[8] So far, however, the microstructures of BHJ films have largely been empirically manipulated by controlling coating[5] and postprocessing conditions[5,9−12] of the active organic layer.

In contrast, block copolymers can self-assemble into domains with dimensions on the order of the exciton diffusion length (L_d ~20 nm), and thus many groups have synthesized semiconducting block copolymers with the aim to control systematically the morphology of active layers in OPVs.[13,14] The phase behavior of P3AT-containing block copolymers is consequently of increasing interest.[15−27] Obtaining long-range, well-ordered microstructures in diblock and triblock copolymers composed of polythiophene and a coil-like polymer has proven difficult to achieve in practice. To date, only poly(3-hexylthiophene)-*b*-poly(2-vinylpyridine) (P3HT−P2VP) has been shown to form well ordered microstructures, and this occurred only after specific solvent annealing conditions were employed.[19] Generally, the lack of long-range order is attributed to the crystallization of the highly regioregular polythiophene moiety; crystallization dominates the phase behavior. The regioregular, semicrystalline polythiophenes generated by the Grignard metathesis (GRIM) method[28,29] are desirable due to their enhanced optoelectronic properties relative to their regiorandom, noncrystalline counterparts. However, amorphous (or low melting temperature) polythiophenes may prove more useful in generating ordered block copolymer microstructures, as has been the case with PPV-based rod−coil block copolymers.[30−34]

Here we report the synthesis of polylactide-*b*-polythiophene-*b*-polylactide block copolymers (PLA−PT−PLA) by the controlled polymerization of D,L-lactide[35−37] from hydroxyl-terminated telechelic polythiophenes (HO-PT-OH). Polylactide was chosen as it can be selectively etched from a polythiophene matrix to yield a nanoporous film[23] that subsequently could be filled with an electron-accepting material for OPV applications.[38] We synthesized three distinct series of PLA−PT−PLA block copolymers: regioregular poly(3-dodecylthiophene) (PLA-*Re*P3DDT-PLA), regiorandom poly(3-hexylthiophene) (PLA-*Ra*P3HT-PLA), and poly(3-dodecylthiophene-*co*-thiophene) (PLA-*co*PT−PLA). We demonstrate that this general postpolymerization functionalization of regioregular polythiophene homopolymers can be extended to generate regioirregular polythiophenes and thiophene statistical copolymer macroinitiators.

Results and Discussion

The syntheses of the PLA−PT−PLA triblock copolymers are shown in Scheme 1. The synthetic strategy utilized to generate the hydroxyl-functionalized polythiophenes is similar to that previously outlined by Liu and McCullough.[39] Here, we have expanded this protocol to include nonregioregular polythiophenes and have used the HO-PT-OH macroinitiators to generate ABA-type triblock copolymers.[40] The polythiophene midblocks incorporate specific physical properties into the triblocks. Regioregular poly(3-dodecylthiophene) was chosen because the melting temperature of the more common regioregular P3HT is above the thermal degradation temperature polylactide; thus, the use of P3DDT allowed annealing of the PLA-*Re*P3DDT-PLA block copolymers above the melting temperature of P3DDT but below the degradation temperature of PLA.[23,41] In the regiorandom midblock case, we chose poly(3-hexylthiophene) even though this block has a larger band gap and ~10% of the hole mobility of regioregular P3HT.[42] On the positive side, phase separation in this block copolymer system would not be influenced by crystallization of the semiconducting block. Previous work with copolymerized thiophene and 3-dodecylthiophene monomers has shown that these materials have little to no crystallinity.[43] Importantly, similar materials to the *co*PT midblock used in this work showed reasonable power conversion efficiencies in typical BHJ solar cells.[43] Thus, PLA-*co*PT-PLA may play an important role in generating well-ordered semiconducting microstructures that are not influenced by crystallization of the midblock but are capable of efficient charge transport.

The end groups of regioregular, regiorandom, and copolymerized P3ATs were converted into nonfunctionalized (i.e., H-terminated) end groups (PT) through the use of the halogen−magnesium exchange reaction followed by hydrolysis. PT polymers were converted to the bis-aldehyde polymers (HCO-PT-COH) using a Vilsmeier transformation[44] and were subsequently reduced with $LiAlH_4$ to the hydroxyl-terminated polythiophenes. HO−PT−OH polymers were used as macroinitiators for the tin octanoate [Sn(oct)$_2$]-catalyzed ring-opening polymerization (ROP) of D,L-lactide[45,46] to give atactic PLA end blocks.[47] Note that *Re*P3DDT- and *Ra*P3HT-based block copolymers have no unsubstituted thiophene repeat units ($m = 0$) while *co*PT has 10 unsubstituted thiophene units on average (m = 10) (see Scheme 1).

---

*To whom correspondence should be addressed. E-mail: frisbie@cems.umn.edu (C.D.F.), hillmyer@umn.edu (M.A.H.).

The PLA chain lengths could be tuned through stoichiometry and conversion. PLA−PT−PLA block copolymers were synthesized from the three parent macroinitiators, HO-*Re*P3DDT-OH, HO-*Ra*P3HT-OH, and HO-*co*PT-OH (Table 1). The molecular weights of the polymers were determined using ^{1}H NMR spectroscopy end-group analysis. *Re*P3DDT and *co*PT were synthesized using the GRIM method, leading to polythiophenes with relatively narrow molecular weight distributions (M_w/M_n) by SEC. However, the mechanism used to generate *Ra*P3HT leads to polythiophenes with polydispersity indices typically greater than 3.[48]

Representative ^{1}H NMR spectra of the PLA−PT−PLA block copolymers are shown in Figure 1; the main-chain polythiophene and polylactide resonances are consistent with our previous report.[23] The inset of Figure 1 illustrates the difference in chemical shift and splitting patterns for the three different types of aromatic protons present in the regioregular, regiorandom, and copolymer thiophene blocks. As expected, the resonances at

Scheme 1. Synthesis of Polylactide−Polythiophene−Polylactide (PLA−PT−PLA)

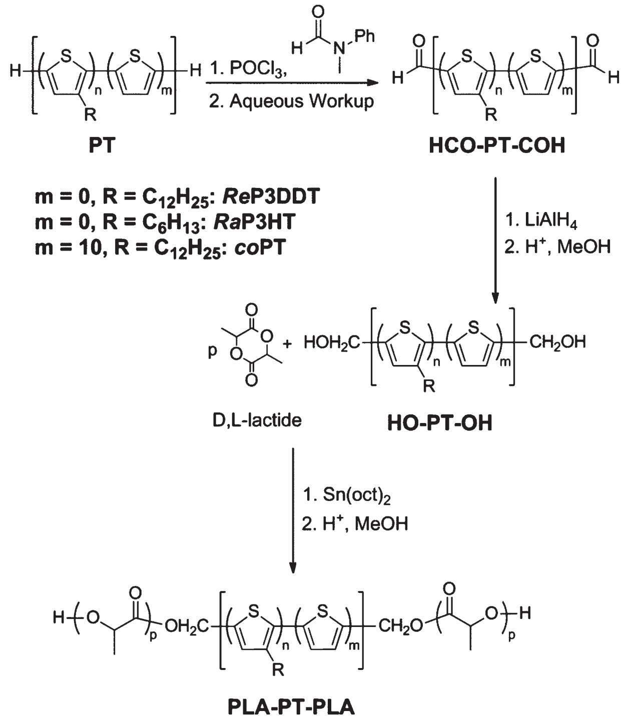

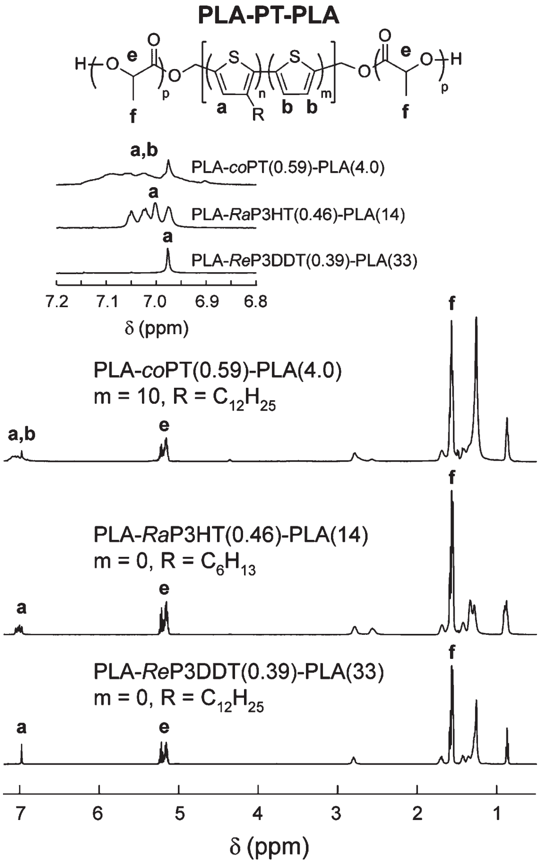

Figure 1. Representative ^{1}H NMR spectra of the PLA-*Re*P3DDT-PLA, PLA-*Ra*P3HT-PLA, and PLA-*co*PT−PLA block copolymer series. The inset shows a magnified view of the region of interest for aromatic protons. The unlabeled peaks upfield of $\delta = 3$ ppm are due to the protons on the alkyl side chains. The polymers were dissolved in deuterated chloroform and spectra were recorded at room temperature.

Table 1. Characterization of PLA−PT−PLA Samples

	M_n[b] (kg/mol)				T_g (°C)		T_m (°C)	
sample[a]	PT	PLA	M_w/M_n[c]	w_{PT}[d]	PT	PLA	PT	crystallinity[f] (%)
HO-*Re*P3DDT-OH	21.0		1.9		−10		156	16
PLA-*Re*P3DDT(0.72)-PLA(8)	21.0	8.1	2.2	0.72	−8	54	157	4
PLA-*Re*P3DDT(0.39)-PLA(33)	21.0	33.1	2.0	0.39	−9	56	160	5
PLA-*Re*P3DDT(0.37)-PLA(35)	21.0	34.6	1.9	0.37	−8	58	159	3
HO-*Ra*P3HT-OH	12.5		4.6		14			
PLA-*Ra*P3HT(0.56)-PLA(11)	12.5	11.0	3.6	0.53	16	48		
PLA-*Ra*P3HT(0.46)-PLA(14)	12.5	14.4	4.4	0.46	17	53		
PLA-*Ra*P3HT(0.35)-PLA(24)	12.5	23.5	4.9	0.35	15	50		
HO-*co*PT-OH	5.8		1.7		25			
PLA-*co*PT(0.82)-PLA(1.3)	5.8	1.3	2.1	0.82	e	39		
PLA-*co*PT(0.77)-PLA(1.7)	5.8	1.7	2.0	0.77	e	41		
PLA-*co*PT(0.59)-PLA(4.0)	5.8	4.0	1.8	0.59	e	45		
PLA-*co*PT(0.14)-PLA(35.7)	5.8	35.7	1.5	0.14	e	50		

[a] HO-*Re*P3DDT-OH is the homopolymer of the polylactide-*b*-regioregular poly(3-dodecylthiophene)-*b*-polylactide series symbolized by PLA-*Re*P3DDT(*X*)-PLA(*Y*), where *X* is the weight fraction of polythiophene present in the polymer and the PLA has a molecular weight of *Y* kg/mol. HO-*Ra*P3HT-OH is the homopolymer of the polylactide-*b*-regiorandom poly(3-hexylthiophene)-*b*-polylactide series symbolized by PLA-*Ra*P3HT(*X*)-PLA(*Y*), where *X* is the weight fraction of polythiophene present in the polymer and the PLA has a molecular weight of *Y* kg/mol. HO-*co*PT-OH is the homopolymer of the polylactide-*b*-poly(3-dodecylthiophene-*co*-thiophene)-*b*-polylactide series symbolized by PLA-*co*PT(*X*)-PLA(*Y*), where *X* is the weight fraction of polythiophene present in the polymer and the PLA has a molecular weight of *Y* kg/mol. [b] As determined by ^{1}H NMR spectroscopy. [c] As determined by SEC versus polystyrene standards. [d] $w_{PT} = M_n(PT)/[M_n(PLA) + M_n(PT)]$. [e] The weak glass transition signal from the polythiophene block is masked by the polylactide block glass transition signal in the *co*PT series of polymers. [f] As determined by the ratio of the enthalpy of melting for the P3DDT fraction of the sample relative to the infinite enthalpy of melting reported in the literature for the P3DDT ($\Delta H_m^\infty = 55$ J/g).[50]

$\delta \approx 2.8$ ppm associated with the α-carbon protons of the alkyl chains also differ between the three types of polythiophene blocks.[48] The end groups of HO-PT-OH macroinitiators and PLA−PT−PLA triblock copolymers were also monitored (Figure S1). The resonance associated with the methylene end group protons at $\delta \approx 4.8$ ppm in HO-PT-OH is no longer observed upon PLA addition presumably because this resonance has approximately the same chemical shift as one of the main chain PLA protons (e in Figure 1, $\delta \approx 5.2$ ppm). Upon addition of PLA, a triplet, corresponding to the terminal repeat units of the PLA chains, at $\delta \approx 4.4$ ppm was observed (Figure S1). Integration of these resonances shows complete conversion of HO-PT-OH to PLA−PT−PLA, which is consistent with clear shifts to higher elution volumes in the SEC data for the triblock copolymers relative to the HO-PT-OH homopolymers (Figure S2).[49] These data indicate that the postpolymerization functionalization and subsequent D,L-lactide polymerization strategy shown in Scheme 1 is robust and can be used to generate a wide variety of polythiophene-based triblock copolymers.

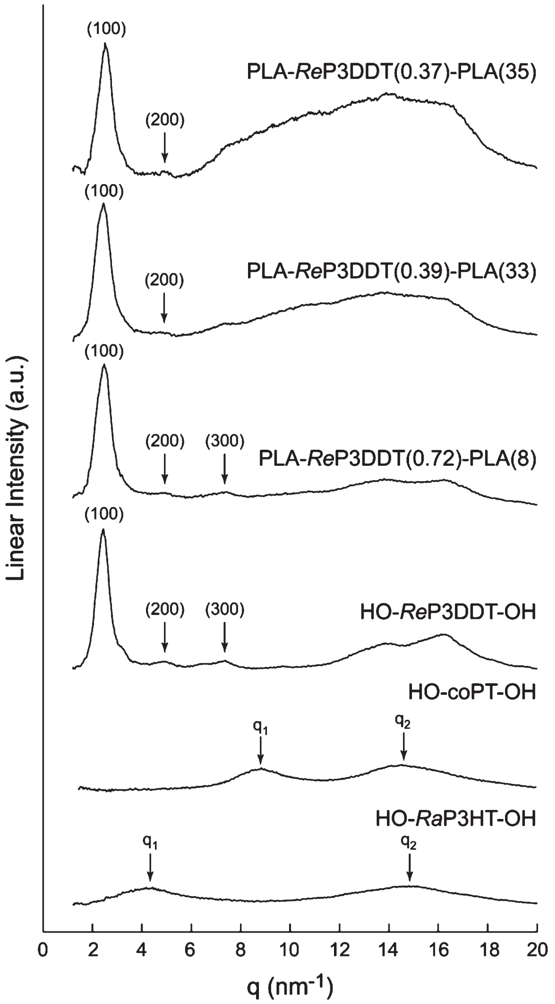

Figure 2. WAXS spectra of the HO-PT-OH homopolymers and the semicrystalline PLA-*Re*P3DDT-PLA triblock copolymers. The prominent lamellae reflections are marked for the semicrystalline samples. Note that all of the *Re*P3DDT samples exhibit sharp, prominent (100) and (200) reflections while the amorphous samples do not; this confirms the lack of melting endotherms in the DSC data. No annealing treatments were performed prior to acquiring these data.

Differential scanning calorimetry (DSC) data showed both main-chain and side-chain melting transitions for the PLA-*Re*P3DDT-PLA series of block copolymers,[50] but no melting transitions were observed for the HO-*Ra*P3HT-OH or HO-*co*PT-OH polymers (Figure S3). This lack of crystalline order was confirmed by wide-angle X-ray scattering (WAXS) experiments. Figure 2 shows that clear (100) and (200) reflections associated with crystalline lamellae (orthogonal to the π-stacking direction) of regioregular poly(3-dodecylthiophene) are present in all of the PLA-*Re*P3DDT-PLA samples, even at 63 wt % PLA. On the other hand, only broad signals are present in the HO-*Ra*P3HT-OH and HO-*co*PT-OH cases indicating amorphous structures. The broad reflections at lower (q_1) and higher (q_2) angles are associated with lamellar and π−π interchain stacking, respectively.[51,52] As expected, the interchain π-stacking spacing is approximately the same for the *Ra*P3HT and *co*PT as the structure of the polythiophene backbone rings remains nearly unchanged between the two cases. However, the q_1 reflection of *Ra*P3HT appears at a lower q value than the *co*PT polymer, which suggests that the lack of alkyl substitution on every thiophene repeat unit allows the polythiophene lamellae to pack closer together in the copolymerized thiophene case.

Preliminary thin film studies imply that the composition of the polythiophene block can influence the microstructures observed using atomic force microscopy (Figure 3). PLA-*co*PT(0.82)-PLA(1.3) and PLA-*co*PT(0.77)-PLA(1.7) self-assembled into lamellar-like structures. However, the thin film of PLA-*co*PT-(0.14)-PLA(35.7) shows phase-separated domains with curved interfaces on the order of the exciton diffusion length (Figure 3c). These results suggest that the synthesis of block copolymers containing regiorandom or copolymerized thiophenes and a sacrificial block could be useful in developing polythiophene

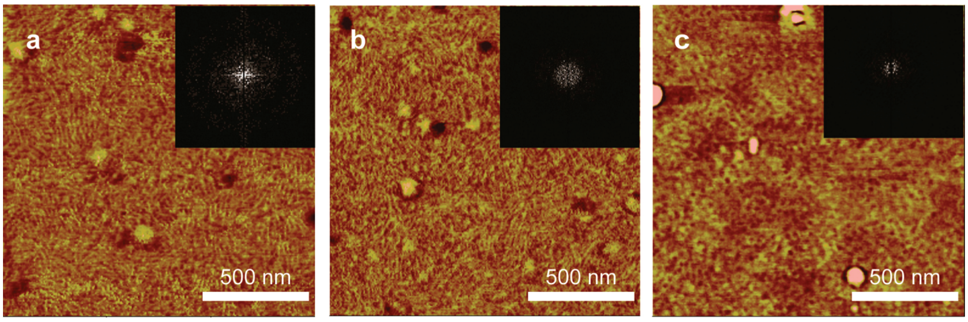

Figure 3. AFM thin film phase images of (a) PLA-*co*PT(0.82)-PLA(1.3), (b) PLA-*co*PT(0.77)-PLA(1.7), and (c) PLA-*co*PT(0.14)-PLA(35.7). The insets show the fast Fourier transforms (FFTs) of the acquired phase images. Integration of the FFTs indicated domain spacings of 20, 21, and 19 nm for images a, b, and c, respectively. The AFM image (not shown) acquired for PLA-*co*PT(0.59)-PLA(4.0) had no discernible domain spacing. The films were spun-coat from 10 mg of polymer in 1 mL of 1,2-dichlorobenzene solutions onto glass substrates at a rotation rate of 1000 rpm for 1 min. Final film thicknesses were all 20 ± 4 nm as measured by AFM. The films were annealed at 150 °C in inert atmosphere for 10 min. The phase scale for (a) and (c) is 20°, and the phase scale for (b) is 15°. The RMS roughness value for the glass substrates was ~1.5 nm over a $10 \times 10\,\mu m^2$ area, as measured using the AFM.

films for ordered bulk heterojunction photovoltaics where the microstructures are not dominated by the crystallization of the polythiophene moiety.

Conclusions

We have demonstrated the synthesis of polylactide-*b*-polythiophene-*b*-polylactide triblock copolymers from a variety of difunctional polythiophene-based macroinitiators. This protocol was applicable to polythiophene blocks with differing regiochemistries and comonomer contents. DSC and powder X-ray scattering indicated the regiorandom poly(3-hexylthiophene) and copolymerized poly(3-dodecyl-*co*-thiophene) macroinitiators were amorphous. Initial studies suggest that block copolymers synthesized from regiorandom or copolymerized polythiophenes phase separate into morphologies not dominated by the crystallization of the polythiophene block, as opposed to the case of block copolymers containing a regioregular polythiophene moiety. This phase behavior could prove useful in controlling the long-range microstructures of the active layers in organic photovoltaic devices.

Acknowledgment. This work was funded by the Initiative for Renewable Energy and the Environment (IREE) at the University of Minnesota and the Xcel Renewable Development Fund. Parts of this work were carried out in the University of Minnesota IT Characterization Facility, which receives partial support from the NSF through the NNIN program. We thank Derek M. Stevens for substrate surface roughness measurements and helpful discussions.

Supporting Information Available: ^{1}H NMR spectroscopy end-group analysis of polythiophene macroinitiators and block copolymers, SEC chromatograms for the macroinitiators and block copolymers, DSC thermograms, and detailed synthetic procedures. This material is available free of charge via the Internet at http://pubs.acs.org.

References and Notes

(1) Skotheim, T., Reynolds, J., Elsembauer, R., Eds. *Handbook of Conducting Polymers*; Marcel Dekker: New York, 1998.
(2) Nalwa, H. S., Ed. *Handbook of Organic Conductive Molecules and Polymers*; J. Wiley & Sons: New York, 1996.
(3) McCullough, R. D. *Adv. Mater.* **1998**, *10*, 93–116.
(4) Osaka, I.; McCullough, R. D. *Acc. Chem. Res.* **2008**, *41*, 1202–1214.
(5) Li, G.; Shrotriya, V.; Huang, J.; Yao, Y.; Moriarty, T.; Emery, K.; Yang, Y. *Nat. Mater.* **2005**, *4*, 864–868.
(6) Ma, W.; Yang, C.; Gong, X.; Lee, K.; Heeger, A. J. *Adv. Funct. Mater.* **2005**, *15*, 1617–1622.
(7) Park, S. H.; Roy, A.; Beaupré, S.; Cho, S.; Coates, N.; Moon, J. S.; Moses, D.; Leclerc, M.; Lee, K.; Heeger, A. J. *Nat. Photonics* **2009**, *3*, 297–303.
(8) Thompson, B. C.; Fréchet, J. M. J. *Angew. Chem., Int. Ed.* **2008**, *47*, 58–77.
(9) Schilinsky, P.; Waldauf, C.; Brabec, C. J. *Appl. Phys. Lett.* **2002**, *81*, 3885–3887.
(10) Padinger, F.; Rittberger, R. S.; Sariciftci, N. S. *Adv. Funct. Mater.* **2003**, *13*, 85–88.
(11) Erb, T.; Zhokhavets, U.; Gobsch, G.; Raleva, S.; Stühn, B.; Schilinsky, P.; Waldauf, C.; Brabec, C. J. *Adv. Funct. Mater.* **2005**, *15*, 1193–1196.
(12) Clarke, T. M.; Ballantyne, A. M.; Nelson, J.; Bradley, D. D. C.; Durrant, J. R. *Adv. Funct. Mater.* **2008**, *18*, 4029–4035.
(13) Segalman, R. A.; McCulloch, B.; Kirmayer, S.; Urban, J. J. *Macromolecules* **2009**, *42*, 9205–9216.
(14) Darling, S. B. *Energy Environ. Sci.* **2009**, *2*, 1266–1273.
(15) Liu, J.; Sheina, E.; Kowalewski, T.; McCullough, R. D. *Angew. Chem., Int. Ed.* **2002**, *41*, 329–332.
(16) Tu, G.; Li, H.; Forster, M.; Heiderhoff, R.; Balk, L. J.; Scherf, U. *Macromolecules* **2006**, *39*, 4327–4331.
(17) Iovu, M. C.; Jeffries-EL, M.; Zhang, R.; Kowalewski, T.; McCullough, R. D. *J. Polym. Sci., Part A* **2006**, *43*, 1991–2000.
(18) Sauvé, G.; McCullough, R. D. *Adv. Mater.* **2007**, *19*, 1822–1825.
(19) Dai, C.; Yen, W.; Lee, Y.; Ho, C.; Su, W. *J. Am. Chem. Soc.* **2007**, *129*, 11036–11038.
(20) Iovu, M. C.; Craley, R.; Jeffries-EL, M.; Krankowski, A. B.; Zhang, R.; Kowalewski, T.; McCullough, R. D. *Macromolecules* **2007**, *40*, 4733–4735.
(21) Sommer, M.; Lang, A. S.; Thelakkat, M. *Angew. Chem., Int. Ed.* **2008**, *47*, 7901–7904.
(22) Richard, F.; Brochon, C.; Leclerc, N.; Eckhardt, D.; Heiser, T.; Hadziioannou, G. *Macromol. Rapid Commun.* **2008**, *29*, 885–891.
(23) Boudouris, B. W.; Frisbie, C. D.; Hillmyer, M. A. *Macromolecules* **2008**, *41*, 67–75.
(24) Higashihara, T.; Ohshimizu, K.; Hirao, A.; Ueda, M. *Macromolecules* **2008**, *41*, 9505–9507.
(25) Urien, M.; Erothu, H.; Cloutet, E.; Hiorns, R. C.; Vignau, L.; Cramail, H. *Macromolecules* **2008**, *41*, 7033–7040.
(26) Higashihara, T.; Ueda, M. *React. Funct. Polym.* **2009**, *69*, 457–462.
(27) Zhang, Q.; Cirpan, A.; Russell, T. P.; Emrick, T. *Macromolecules* **2009**, *42*, 1079–1082.
(28) Loewe, R. S.; Khersonsky, S. M.; McCullough, R. D. *Adv. Mater.* **1999**, *11*, 250–253.
(29) Jeffries-EL, M.; Sauvé, G.; McCullough, R. D. *Adv. Mater.* **2004**, *16*, 1017–1019.
(30) Olsen, B. D.; Segalman, R. A. *Macromolecules* **2005**, *38*, 10127–10137.
(31) Olsen, B. D.; Segalman, R. A. *Macromolecules* **2006**, *39*, 7078–7083.
(32) Olsen, B. D.; Li, X.; Wang, J.; Segalman, R. A. *Macromolecules* **2007**, *40*, 3287–3295.
(33) Ho, C. C.; Lee, Y. H.; Dai, C. A.; Segalman, R. A.; Su, W. F. *Macromolecules* **2009**, *42*, 4208–4219.
(34) Olsen, B. D.; Segalman, R. A. *Mater. Sci. Eng., R* **2008**, *62*, 37–66.
(35) Schmidt, S. C.; Hillmyer, M. A. *Macromolecules* **1999**, *32*, 4794–4801.
(36) Kricheldorf, H.; Berl, M.; Scharnagle, N. *Macromolecules* **1988**, *21*, 286–293.
(37) Wang, Y.; Hillmyer, M. A. *Macromolecules* **2000**, *33*, 7395–7403.
(38) Botiz, I.; Darling, S. B. *Macromolecules* **2009**, *42*, 8211–8217.
(39) Liu, J.; McCullough, R. D. *Macromolecules* **2002**, *35*, 9882–9889.
(40) Full experimental details for the thiophene polymerizations, end-functionalizations, and lactide polymerizations are described in the Supporting Information.
(41) Olayo-Valles, R.; Guo, S.; Lund, M. S.; Leighton, C.; Hillmyer, M. A. *Macromolecules* **2005**, *38*, 10101–10108.
(42) Pandey, S. S.; Takashima, W.; Nagamatsu, S.; Endo, T.; Rikukawa, M.; Kaneto, K. *Jpn. J. Appl. Phys.* **2000**, *39*, L94–L97.
(43) Thompson, B. C.; Kim, B. J.; Kavulak, D. F.; Sivula, K.; Mauldin, C.; Fréchet, J. M. J. *Macromolecules* **2007**, *40*, 7425–7428.
(44) Witiak, D. T.; Williams, D. R.; Kakodkar, S. V. *J. Org. Chem.* **1974**, *39*, 1242–1247.
(45) Kricheldorf, H. R.; Kreiser-Saunders, I.; Stricker, A. *Macromolecules* **2000**, *33*, 702–709.
(46) Ryner, M.; Stridsberg, K.; Albertsson, A. C.; von Schenck, H.; Svensson, M. *Macromolecules* **2001**, *34*, 3877–3881.
(47) Li, S. *J. Biomed. Mater. Res.* **1999**, *48*, 342–353.
(48) Chen, T. A.; Wu, X.; Rieke, R. D. *J. Am. Chem. Soc.* **1995**, *117*, 233–244.
(49) The rod−coil nature of the block copolymers causes retention volume shifts to be lower than expected for all three series of block copolymers. The large polydispersity of the polythiophene block in the PLA-*Ra*P3HT-PLA polymers also hinders the ability to easily observe a clear shift in elution volume. We note that the PLA-*co*PT(0.14)-PLA(35.7) contains a trace amount ($< 10\%$) of polythiophene homopolymer.
(50) Malik, S.; Nandi, A. K. *J. Polym. Sci., Part B* **2002**, *40*, 2073–2085.
(51) Prosa, T. J.; Winokur, M. J.; Moulton, J.; Smith, P.; Heeger, A. J. *Macromolecules* **1992**, *25*, 4364–4372.
(52) Sirringhaus, H.; Brown, P. J.; Friend, R. H.; Nielsen, M. M.; Bechgaard, K.; Langeveld-Voss, B. M. W.; Spiering, A. J. H.; Janssen, R. A. J.; Meijer, E. W.; Herwig, P.; de Leeuw, D. M. *Nature* **1999**, *401*, 685–688.